



ELSEVIER

Journal of Nuclear Materials 282 (2000) 83–88

Journal of  
nuclear  
materials

www.elsevier.nl/locate/jnucmat

Letter to the Editors

# Embrittlement of low copper VVER 440 surveillance samples neutron-irradiated to high fluences <sup>☆</sup>

M.K. Miller <sup>a,\*</sup>, K.F. Russell <sup>a</sup>, J. Kocik <sup>b</sup>, E. Keilova <sup>b</sup>

<sup>a</sup> *Microscopy and Microanalytical Sciences Group, Metals and Ceramics Division, Oak Ridge National Laboratory, Building 4500 S, MS 6136, P.O. Box 2008, Oak Ridge, TN 37831-6136, USA*

<sup>b</sup> *Nuclear Research Institute Rez plc, 250 68 Rez Prague, Czech Republic*

Received 24 March 2000; accepted 22 May 2000

## Abstract

An atom probe tomography microstructural characterization of low copper (0.06 at.% Cu) surveillance samples from a VVER 440 reactor has revealed manganese and silicon segregation to dislocations and other ultrafine features in neutron-irradiated base and weld materials (fluences  $1 \times 10^{25} \text{ m}^{-2}$  and  $5 \times 10^{24} \text{ m}^{-2}$ ,  $E > 0.5 \text{ MeV}$ , respectively). The results indicate that there is an additional mechanism of embrittlement during neutron irradiation that manifests itself at high fluences. © 2000 Published by Elsevier Science B.V. All rights reserved.

## 1. Introduction

It is economically desirable to extend the service life of nuclear reactors. One of the limiting factors is the embrittlement of the pressure vessel due to the interaction of the solutes in the vessel with the vacancies and other products created by the incident neutrons. In order to extend the lifetime of the reactor, it is essential to be able to predict the changes that will occur in the microstructure of the steel and their consequences on the mechanical properties.

Previous atom probe experiments on both Western and Russian type steels have revealed that the matrix copper content was reduced to  $\sim 0.05 \text{ at.}\%$  Cu after neutron irradiation to fluences in the low  $10^{23} \text{ m}^{-2}$  and that this reduction was accompanied by the formation of copper-enriched precipitates [1]. This matrix copper level

was found to be reduced slightly by annealing the steels for 168 h at  $454^\circ\text{C}$ . Therefore, it has been proposed that the embrittlement may be reduced or eliminated through the use of low copper steels. Examination of the embrittlement database (EDB) of mechanical properties from low copper ( $< 0.06\%$ ) neutron-irradiated pressure vessel steels reveals that the maximum shift in the ductile-to-brittle transition temperature is of the order of  $30^\circ\text{C}$ ; however, the range of fluences examined is limited to less than  $6 \times 10^{23} \text{ m}^{-2}$  ( $E > 1 \text{ MeV}$ ) [2,3].

In this study, an atomic level microstructural characterization has been performed on low copper surveillance specimens that were exposed to high fluences in a VVER 440 reactor in order to evaluate the susceptibility of low copper reactor pressure vessel steels to embrittlement.

## 2. Materials and experimental conditions

The compositions of the 15Kh2MFA base and 10KhMFT weld specimens used in this study are given in Table 1. The copper level in these materials is  $\sim 0.06 \text{ at.}\%$  Cu. The nickel content of the base material,  $0.07 \text{ at.}\%$ , was significantly lower than that present ( $\sim 0.5 \text{ at.}\%$  Ni) in typical A533B type steels. There was

<sup>☆</sup> The submitted manuscript has been authored by a contractor of the US Government under contract No. DE-AC05-96OR22464. Accordingly, the US Government retains a nonexclusive, royalty-free license to publish or reproduce the published form of this contribution, or allow others to do so, for US Government purposes.

\* Corresponding author. Tel.: +1-865 574 4719; fax: +1-865 574 0641.

E-mail address: millermk@ornl.gov (M.K. Miller).

Table 1  
Compositions of the base (15Kh2MFAA) and weld (10KhMFT) materials<sup>a</sup>

| Element | Base material (15Kh2MFAA) |          | Weld material (10KhMFT) |          |
|---------|---------------------------|----------|-------------------------|----------|
|         | Mass %                    | Atomic % | Mass %                  | Atomic % |
| Cu      | 0.07                      | 0.06     | 0.06                    | 0.05     |
| Cr      | 2.9                       | 3.1      | 1.37                    | 1.46     |
| Mo      | 0.66                      | 0.35     | 0.5                     | 0.29     |
| Mn      | 0.46                      | 0.46     | 1.1                     | 1.11     |
| V       | 0.31                      | 0.34     | 0.2                     | 0.22     |
| Ni      | 0.07                      | 0.07     | –                       | –        |
| Si      | 0.17                      | 0.34     | 0.59                    | 1.17     |
| C       | 0.16                      | 0.74     | 0.037                   | 0.17     |
| S       | 0.016                     | 0.028    | 0.017                   | 0.029    |
| P       | 0.014                     | 0.025    | 0.012                   | 0.02     |
| N       | 0.008                     | 0.028    | 0.018                   | 0.071    |
| O       | 0.0039                    | 0.013    | 0.081                   | 0.32     |

<sup>a</sup> The balance is iron.

no nickel in the weld. All compositions are given in atomic percent.

The base material was initially annealed at 1000°C and quenched into oil at 125°C. The base material was characterized (1) after tempering for 18 h at 690°C plus a simulated stress relief treatment of 6 + 6 + 11 + 10.5 h at 680°C, (2) after neutron irradiation at 270°C for 10 yr to a fluence of  $1.0 \times 10^{25} \text{ m}^{-2}$  ( $E > 0.5 \text{ MeV}$ , flux =  $3.8 \times 10^{16} \text{ m}^{-2} \text{ s}^{-1}$ ) and (3) after thermal aging for 10 yr at 295°C. These treatments will be referred to as unirradiated, neutron-irradiated and thermally aged conditions, respectively. The weld material was also examined (1) after welding and stress relief treatment 6 + 6 + 11 + 10.5 h at 680°C, (2) after neutron irradiation at 275°C for 5 yr to a fluence of  $5.2 \times 10^{24} \text{ m}^{-2}$  ( $E > 0.5 \text{ MeV}$ , flux =  $3.8 \times 10^{16} \text{ m}^{-2} \text{ s}^{-1}$ ) and (3) after thermal aging for 5 yr at 295°C. These fluences are equivalent to  $\sim 6.6 \times 10^{24} \text{ m}^{-2}$  ( $E > 1 \text{ MeV}$ ) and  $\sim 3.5 \times 10^{24} \text{ m}^{-2}$  ( $E > 1 \text{ MeV}$ ) for the base and weld metals, respectively and are both significantly higher than the typical end of life fluence of  $\sim 3 \times 10^{23} \text{ m}^{-2}$  ( $E > 1 \text{ MeV}$ ).

In both materials, the samples were irradiated in positions for surveillance specimens in vertical channels welded to the outer surface of the core barrel of the VVER-440 reactor. The neutron fluences for the base and weld Charpy V-notch specimens were 9.3 and  $5.2 \times 10^{24} \text{ m}^{-2}$  ( $E > 0.5 \text{ MeV}$ ), respectively. These fluences were slightly different from the atom probe specimens due to their different positions in the surveillance capsules.

The microstructures of the materials were characterized in the Oak Ridge energy-compensated optical position-sensitive atom probe (ECOPOSAP) [4]. Specimens were fabricated from electropolished small bars cut from Charpy V-notch samples [4]. All atom probe analyses were performed with a specimen temperature of

50 K, a pulse fraction of 20% and a pulse repetition rate of 1500 Hz.

### 3. Results and discussion

The microstructure of the base metal was classified as a mixture of tempered granular and lath bainite, with a small amount of ferrite [5]. The microstructure of the weld metal was found to consist predominantly of acicular ferrite with a small amount of bainite and a network of proeutectoid ferrite. The dislocation density was determined to be 2.3 and  $1.5 \times 10^{14} \text{ m}^{-2}$  for the unirradiated base and weld metals, respectively. Blocky chromium-rich  $\text{M}_7\text{C}_3$  and  $\text{M}_{23}\text{C}_6$  type precipitates, typically 200 nm in size, were located preferably along boundaries. An atom probe analysis of a  $\text{M}_7\text{C}_3$  carbide in the thermally aged base material yielded a composition of  $41.7 \pm 2.0\%$  Cr,  $23.1 \pm 1.5\%$  Fe,  $3.4 \pm 0.6\%$  V,  $1.7 \pm 0.4\%$  Mn,  $0.3 \pm 0.17\%$  Mo,  $0.3 \pm 0.17\%$  Si + N, and  $29.5 \pm 1.7\%$  C. No phosphorus was found in this carbide. In addition, fine plate-like VC carbides, ranging from  $\sim 5$  to  $\sim 10$  nm in size, were found to be distributed homogeneously within the microstructure in both base and weld metals. The average compositions of these precipitates are given in Table 2. Phosphorus segregation was evident at the precipitate–matrix interface.

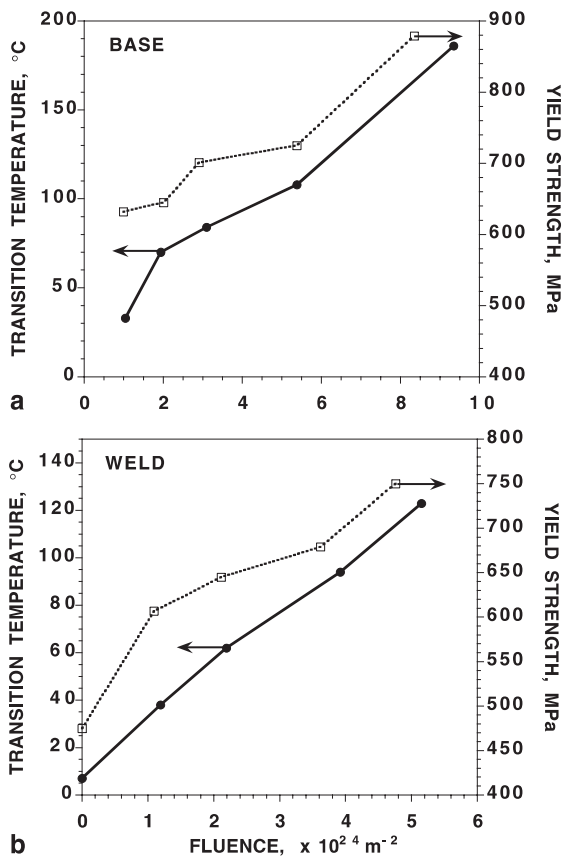
Transmission electron microscopy of the irradiated materials revealed ‘black dots’, small dislocation loops, fine precipitates concentrated on dislocations and low-angle boundaries [6,7].

A comparison of the tensile and Charpy V-notch test results indicates that the unirradiated and thermally aged materials were similar for the base and weld materials. However, significant increases in the ductile-to-brittle transition temperature (DBTT), yield and ultimate tensile strengths and reductions in the elongation

Table 2

Compositions of vanadium carbide precipitates as determined by atom probe field ion microscopy<sup>a</sup>

| Material                     | V          | Cr        | Mo        | Fe          | C          | N         |
|------------------------------|------------|-----------|-----------|-------------|------------|-----------|
| Thermally aged base material | 40.6 ± 1.8 | 9.3 ± 0.9 | 4.9 ± 0.6 | 0.24 ± 0.14 | 42.9 ± 1.9 | 2.1 ± 0.4 |
| Unirradiated weld            | 40.2 ± 2.6 | 8.9 ± 1.2 | 9.2 ± 1.2 | 1.1 ± 0.4   | 36.8 ± 2.5 | 3.6 ± 0.8 |
| Thermally aged weld          | 42.0 ± 2.7 | 6.5 ± 1.1 | 4.2 ± 0.9 | 2.3 ± 0.6   | 36.7 ± 2.5 | 8.4 ± 1.2 |

<sup>a</sup> The results are in atomic percent.Fig. 1. Change in the transition temperature and yield strength of the: (a) 15Kh2MFA base metal and (b) 10KhMFT weld material as a function of neutron fluence ( $E > 0.5$  MeV).

and reduction in area were observed in base and weld materials after neutron irradiation [7]. For example, the transition temperatures of the base metal were  $-49^{\circ}\text{C}$ ,  $-70^{\circ}\text{C}$  and  $141^{\circ}\text{C}$ , for the unirradiated, thermally aged and neutron-irradiated conditions, respectively. Similarly, the transition temperatures of the weld metal were  $7^{\circ}\text{C}$ ,  $11^{\circ}\text{C}$  and  $123^{\circ}\text{C}$ , respectively, for these three conditions. The gradual increase in the transition temperature and the yield strength as a function of fluence are shown in Figs. 1(a) and (b) for the base and weld metals, respectively. Similar behavior has previously been observed in 15Kh2MFA base and weld metal irradiated to fluences of  $6 \times 10^{24} \text{ m}^{-2}$ ,  $E > 0.5$  MeV [8]. The changes in the rates of increases may indicate that more than one mechanism is responsible for the embrittlement.

Atom probe analysis of the matrix compositions of the three conditions in both materials revealed no significant differences as shown in Table 3 [9]. In particular, the copper content of the matrix was observed to be similar to the bulk composition. In addition, the intragranular copper-enriched precipitates detected in other higher copper pressure vessel steels after irradiation were not observed in these materials [1].

Atom maps of the solute distribution in the neutron-irradiated weld materials, shown in Figs. 2 and 3, respectively, clearly reveal the presence of manganese- and silicon-enriched features in the matrix. Similar features were observed in the neutron-irradiated base material. However, these features were not observed in the stress-relieved or thermally aged materials. Two distinct morphologies were observed in both materials: roughly spherical and roughly cylindrical each having a characteristic diameter of  $\sim 3\text{--}4$  nm. Three-dimensional atom

Table 3

Average compositions of the matrix as determined by atom probe field ion microscopy and atom probe tomography<sup>a</sup>

|    | Base material (15Kh2MFA) |                |                    | Weld material (10KhMFT) |                |                    |
|----|--------------------------|----------------|--------------------|-------------------------|----------------|--------------------|
|    | Unirradiated             | Thermally aged | Neutron-irradiated | Unirradiated            | Thermally aged | Neutron-irradiated |
| Cu | 0.06 ± 0.02              | 0.05 ± 0.02    | 0.06 ± 0.009       | 0.05 ± 0.01             | 0.05 ± 0.006   | 0.05 ± 0.009       |
| Cr | 1.82 ± 0.12              | 2.47 ± 0.20    | 2.19 ± 0.05        | 1.29 ± 0.05             | 1.13 ± 0.03    | 1.33 ± 0.04        |
| Mo | 0.29 ± 0.05              | 0.39 ± 0.08    | 0.31 ± 0.02        | 0.30 ± 0.02             | 0.23 ± 0.01    | 0.37 ± 0.02        |
| Mn | 0.32 ± 0.05              | 0.51 ± 0.09    | 0.31 ± 0.02        | 0.88 ± 0.04             | 1.00 ± 0.02    | 1.08 ± 0.04        |
| V  | 0.10 ± 0.02              | 0.23 ± 0.06    | 0.15 ± 0.01        | 0.08 ± 0.01             | 0.04 ± 0.006   | 0.08 ± 0.01        |
| Si | 0.52 ± 0.06              | 0.34 ± 0.07    | 0.16 ± 0.01        | 1.21 ± 0.05             | 1.19 ± 0.03    | 1.22 ± 0.04        |
| C  | 0.017 ± 0.017            | 0              | 0.17 ± 0.01        | 0.03 ± 0.01             | 0.05 ± 0.06    | 0.17 ± 0.02        |
| P  | 0.017 ± 0.017            | 0.033 ± 0.033  | 0.037 ± 0.006      | 0.04 ± 0.01             | 0.012 ± 0.003  | 0.039 ± 0.003      |

<sup>a</sup> The balance is iron and the results are in atomic percent with a  $2\sigma$  error.

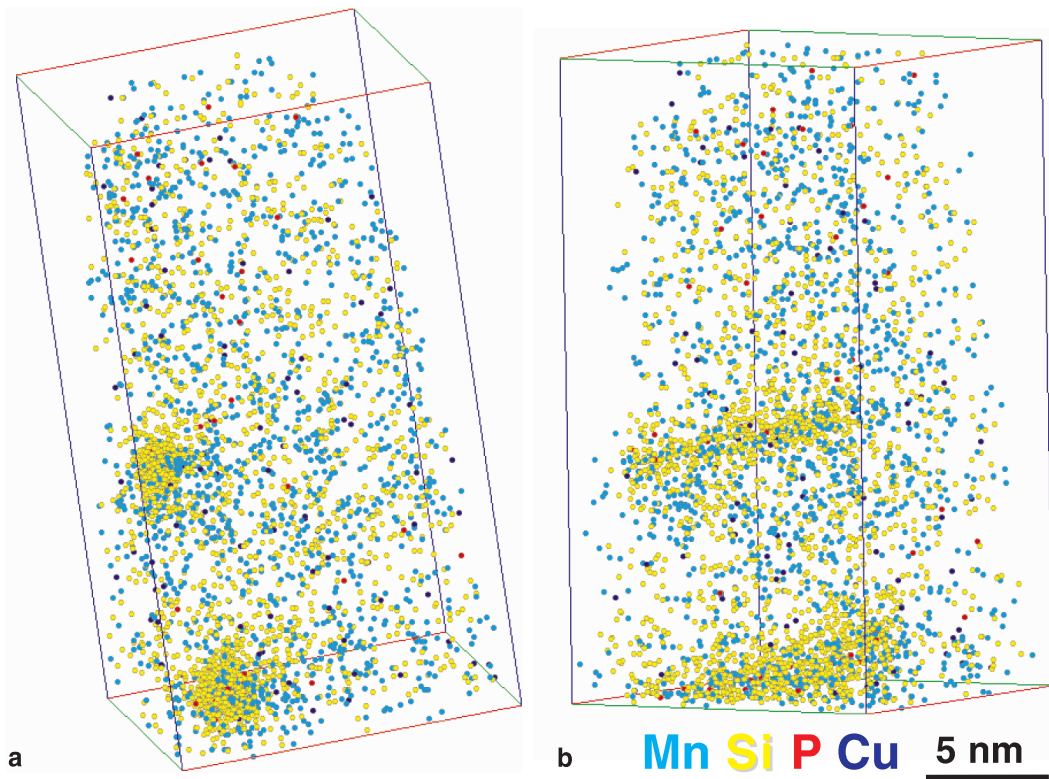


Fig. 2. Atom maps of the solute distribution in the neutron-irradiated weld material. Two cylindrical Ni- and Si-enriched regions are evident. End view of dislocation is shown in (a). The volume has been rotated  $\sim 90^\circ$  about the vertical axis in (b) to show the side view of the dislocation.

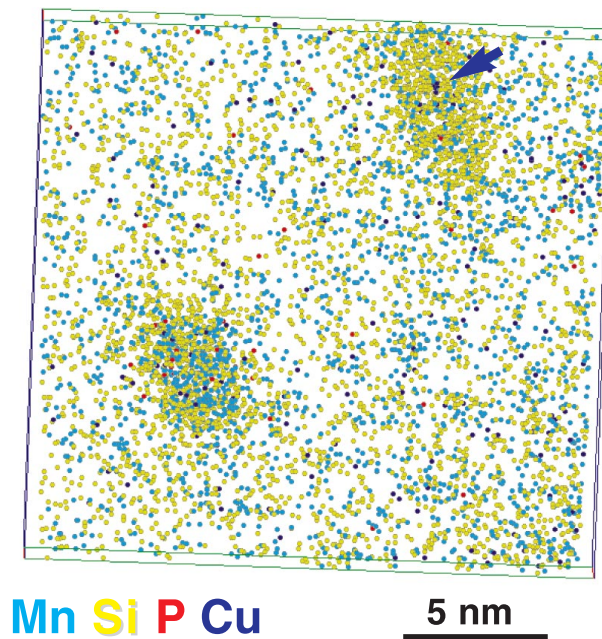


Fig. 3. Atom maps of the solute distribution in the neutron-irradiated weld material. Two spherical Mn- and Si-enriched regions are evident.

Table 4

Compositions of the Mn- and Si-enriched features in neutron-irradiated base and weld materials<sup>a</sup>

|      |   | <i>Cu</i> | <i>Cr</i> | <i>Mo</i> | <i>Mn</i> | <i>V</i> | <i>Si</i> | <i>C</i> | <i>P</i> | Shape    |
|------|---|-----------|-----------|-----------|-----------|----------|-----------|----------|----------|----------|
| Base | F | 0.79      | 2.36      | 0.09      | 3.40      | –        | 15.4      | –        | –        | Sphere   |
|      | G | 0.46      | 3.68      | 0.13      | 2.50      | 0.07     | 4.14      | 0.13     | 0.13     | Sphere   |
|      | H | 0.23      | 2.57      | 0.38      | 2.80      | 0.15     | 3.03      | 0.38     | 0.30     | Cylinder |
| Weld | A | 0.46      | 0.31      | 1.55      | 14.5      | 0.08     | 14.4      | –        | 3.79     | Sphere   |
|      | B | 0.56      | 0.56      | 0.79      | 12.1      | –        | 12.7      | –        | 0.56     | Sphere   |
|      | C | 0.82      | 0.09      | 0.37      | 2.20      | –        | 16.7      | –        | 0.09     | Sphere   |
|      | D | 0.29      | 0.05      | 1.29      | 3.68      | 0.05     | 11.5      | 0.14     | 0.19     | Cylinder |
|      | E | 0.04      | 0.35      | 1.43      | 4.62      | –        | 12.0      | 0.09     | 0.48     | Cylinder |

<sup>a</sup> The balance is iron and the results are in atomic percent.

probe compositional measurements revealed enrichments of manganese, silicon, phosphorus, copper and carbon in the central regions of these features, as shown in Table 4. These figures correspond to enrichment factors of 7–47× for manganese, 12–104× for silicon, 3–115× for phosphorus, up to 16× for copper and up to 2× for carbon. Only a small reduction in solute from the matrix would be required to account for these solute enrichments and therefore, no significant change in the matrix composition would be measured at distances removed from these features. One explanation for the extended cylindrical morphology is solute segregation, possibly through a solute-vacancy drag mechanism, which results in the formation of Cottrell atmospheres in the stress fields associated with dislocations. Similar cylindrical morphology features have been identified as Cottrell atmospheres in boron-doped FeAl [10,11]. There is some experimental evidence that the distribution of solute around the feature is not uniform and that the silicon and manganese are located in different regions of the feature. This non-uniform solute distribution would be expected because the silicon atoms are undersized and manganese atoms are oversized compared to iron atoms, and hence they would be accommodated more efficiently in different regions of the stress field. It is also possible that some of the spherical features could arise from solute segregation to small dislocation loops or other small defects, such as vacancy clusters or nanovoids. Similar silicon-, manganese- and nickel-enriched features have been observed in neutron-irradiated ( $1.2 \times 10^{24} \text{ m}^{-2}$  ( $E > 1 \text{ MeV}$ ), 0.09% Cu) material from the CHOOZ A reactor [12]. Another possibility is that some of the spherical features initially form through the clustering or precipitation of copper atoms and these embryos then attract or act as a sink for the other solutes or vacancies. A  $\sim 5$  atom copper core has been observed in some of the features. All these solute-enriched regions will significantly impede the motion of dislocations and thereby account for the observed changes in the mechanical properties at high fluences.

These experimental results clearly demonstrate that low copper pressure vessel steels are susceptible to embrittlement due to neutron irradiation at high fluences. In addition, they suggest that post-irradiation annealing treatments may not remove the susceptibility of the steel to re-embrittlement during further neutron irradiation. In high copper materials, it has been demonstrated that the post-irradiation annealing treatment increases the size and reduces the number density of copper-enriched precipitates and reduces the copper content of the matrix. Therefore, the small quantity of copper remaining in the matrix would produce little re-embrittlement on subsequent irradiation. In low copper materials, annealing treatments are likely to redistribute the manganese and silicon and recover some of the mechanical properties. In both types of materials, the manganese and silicon can segregate to dislocations and produce embrittlement on subsequent irradiation.

#### 4. Conclusions

This study reports the experimental observation of an additional mechanism for embrittlement in steels used in a VVER 440 reactor that were neutron-irradiated to high fluences. Significant increases were found in the DBTT, yield and ultimate tensile strengths and reductions were found in the elongation and reduction in area in both base and weld materials after neutron irradiation. These changes in mechanical properties correlate with the presence of manganese-, silicon-, copper-, phosphorus- and carbon-decorated dislocations and other features in the matrix of the neutron-irradiated base and weld materials.

#### Acknowledgements

Research at the Oak Ridge National Laboratory SHaRE User Facility was sponsored by the Division of

Materials Sciences and Engineering, US Department of Energy, under contract DE-AC05-96OR22464 with Lockheed Martin Energy Research Corporation and by the Office of Nuclear Regulatory Research, US Nuclear Regulatory Commission under inter-agency agreement DOE 1886-N695-3W with the US Department of Energy. The transmission electron microscopy research at the Nuclear Research Institute Rez plc. was sponsored by the Czech Academy of Sciences under the grant No. 106/96/1319.

## References

- [1] M.K. Miller, P. Pareige, M.G. Burke, *Mater. Character* 44 (2000) 235.
- [2] J.A. Wang, F.B.K. Kam, F.W. Stallmann, in: D.S. Gelles, R.K. Nanstad, A.S. Kumar, E.A. Little (Eds.), *Effects of Radiation on Materials*, ASTM STP 1270, American Society of Testing and Materials, West Conshohocken, PA, USA, 1996, pp. 500–521.
- [3] J.A. Wang, *Embrittlement Data Base, Version 1*, NUREG/CR-6506, ORNL/TM-13327, 1997.
- [4] M.K. Miller, *J. Microsc.* 186 (1997) 1.
- [5] J. Kocik, E. Keilova, *Microstructure of Cr–Mo–V reactor pressure vessel steels*, NRI Research Bulletin, Nucleon, 1998, No. 3, Rez, p. 19.
- [6] J. Kocik, E. Keilova, I. Prochazka, J. Cizek, in: M.L. Hamilton, A.S. Kumar, S.T. Rosinski, M.L. Grossbeck (Eds.), *Proceedings of the 19th Symposium on Effects of Radiation on Materials*, Seattle, June 1998, ASTM STP 1366, American Society of Testing and Materials, West Conshohocken, PA, USA, 2000.
- [7] J. Kocik, E. Keilova, J. Cizek, I. Prochazka, *Radiation damage mechanisms in Cr–Mo–V steels*, in: *Metal 2000*, Ninth International Conference on Metallurgy, May 2000, Ostrava, Czech Republic, paper no. 719.
- [8] A.D. Amayev, A.M. Kryukov, V.I. Levit, M.A. Sokolov, in: L.E. Steele (Ed.), *Radiation Embrittlement of Nuclear Reactor Pressure Vessel Steels: An International Review*, vol. 4, ASTM STP 1170, American Society of Testing and Materials, Philadelphia, PA, USA, 1993, p. 9.
- [9] M.K. Miller, K.F. Russell, J. Kocik, E. Keilova, *Micron* (2000) in press.
- [10] D. Blavette, E. Cadel, A. Fraczkiwicz, A. Menand, *Science* 286 (1999) 2317.
- [11] M.K. Miller, *Science* 286 (1999) 2285.
- [12] P. Auger, P. Pareige, M. Akamatsu, D. Blavette, *J. Nucl. Mater.* 225 (1995) 225.